

## Switching times of ferroelectric domains in x-ray-irradiated $\text{KD}_2\text{PO}_4\text{-KH}_2\text{AsO}_4$ monitored by ESR

Roger D. Truesdale,\* Charles P. Poole, Jr., and Horacio A. Farach

*Department of Physics and Astronomy, University of South Carolina, Columbia, South Carolina 29208*

(Received 1 November 1982)

The polarization reversal of a ferroelectric crystal has been monitored for the first time by the technique of electron-spin resonance. This method was employed to study the reversal process in the ferroelectric crystal  $\text{KD}_2\text{PO}_4$  at low temperatures for a series of electric field strengths. The experiments utilized the  $\text{AsO}_4^{4-}$  free radical formed by x-ray irradiation of single crystals of  $\text{KD}_2\text{PO}_4$  that had been doped with 5 mol % of  $\text{KH}_2\text{AsO}_4$ . At low temperatures the lowest-field hyperfine component of the  $\text{AsO}_4^{4-}$  center exhibited a ferroelectric domain splitting. The relative intensities of this lowest-field doublet provided the fractional polarization  $g(t)$  of the crystal that remained unswitched as the polarized state decayed with time  $t$ . For intermediate times,  $g(t)$  followed a power law of the form  $g(t) \sim t^{-a}$  at low temperatures and field strengths. The electric field dependence of the power-law exponent  $a$  was determined for fields between 4.0 and 8.0 kV/cm at 82 K and the temperature dependence was determined in a 4.0-kV/cm field for temperatures from 88 to 113 K. These dependences were found to be  $a(E) \sim e^{\alpha E}$  and  $a(T) \sim e^{-\beta/T}$ , respectively.

### I. INTRODUCTION

Ferroelectricity exists in a crystal that undergoes a structural phase transition at a critical temperature  $T_c$  from a high-temperature nonpolar (paraelectric) phase to a low-temperature polar (ferroelectric) phase. The major characteristic of the ferroelectric phase is the existence of a spontaneous electrical polarization that can be reversed by an external electric field. Information concerning the mechanisms of polarization reversal in ferroelectric materials has previously been obtained by two principal methods. The decay or growth of domains during the reversal process has been studied by the direct optical observation of the domains, while switching time measurements have been made through the detection of a displacement current that flows through the crystal due to the internal rearrangement of molecular dipolar units as the polarization reverses. Reviews of these methods can be found in the books by Fatuzzo and Merz<sup>1</sup> and by Lines and Glass.<sup>2</sup> This paper presents a new method for monitoring the reversal process which uses electron-spin-resonance (ESR) spectroscopy.

Uniaxial ferroelectric single crystals which have passed into the polar phase in the absence of an external electric field are composed of two types of domains that are polarized in opposite directions along the ferroelectric axis.<sup>3</sup> The ESR spectrum of certain paramagnetic centers in such crystals exhibits a "domain splitting" and the two relative intensities of two hyperfine components provide a mea-

sure of the net polarization state of the crystal, or equivalently, the intensity of each component is proportional to the volume taken up by each type of domain. When an external electric field is applied to the sample along the ferroelectric axis, the polarization of the crystal changes with time due to the switching of domains to the direction favored by the field. The fraction of the domains that has switched (or not switched) as a function of time is then reflected by the time dependence of the intensities of the two components of the ESR spectrum of the paramagnetic centers.

The domain splitting that was just described can be observed in the spectra of several paramagnetic defects or impurities in members of the potassium dihydrogen phosphate class of ferroelectric crystals. In particular, evidence of domain switching and hysteresis effects has been obtained from the spectra of free radicals produced by x- or  $\gamma$ -ray irradiation of pure crystals of  $\text{KH}_2\text{PO}_4$  and  $\text{RbH}_2\text{PO}_4(\cdot\text{OPO}_3\text{H}^-)$ ,  $\text{KD}_2\text{PO}_4(\cdot\text{OPO}_3\text{D}^-)$ ,<sup>4,5</sup> and  $\text{KH}_2\text{AsO}_4$  and  $\text{KD}_2\text{AsO}_4(\text{AsO}_4^{4-})$ .<sup>6</sup> Similar spectra have also been detected from radiation-induced radicals in the mixed crystals  $\text{KH}_2\text{PO}_4\text{-KH}_2\text{AsO}_4(\text{AsO}_4^{4-})$ ,<sup>7</sup>  $\text{KH}_2\text{PO}_4\text{-K}_2\text{SeO}_4(\text{SeO}_4^{3-})$ ,<sup>8</sup> and their deuterated analogs.<sup>9</sup> In this work, the ESR techniques for monitoring the switching process over a range of electric field strengths and temperatures are applied to ferroelectric  $\text{KD}_2\text{PO}_4$  by utilizing the ESR spectrum of the  $\text{AsO}_4^{4-}$  ion. In an earlier Report we presented preliminary results of these studies.<sup>10</sup>

$\text{KD}_2\text{PO}_4$  crystallizes at room temperature in the

tetragonal  $I\bar{4}2d$  ( $D_{2d}^{12}$ ) structure<sup>11-13</sup> except at the highest levels of deuteration where a monoclinic phase is observed.<sup>14</sup> In the high-temperature phase, each tetrahedral  $\text{PO}_4$  group is hydrogen bonded to four neighboring  $\text{PO}_4$  groups. The time-averaged position of the deuterium atom is located symmetrically between the two oxygen atoms connected by the bond. In the  $I\bar{4}2d$  tetragonal structure there are two inequivalent  $\text{PO}_4$  tetrahedra. The geometrically inequivalent  $\text{PO}_4$  groups are rotated in opposite directions about the  $c$  axis through angles of approximately  $16^\circ$ . In the ferroelectric phase below 223 K, the symmetry becomes orthorhombic  $Fdd2$  ( $C_{2v}^{19}$ ) with the orthorhombic  $X$  and  $Y$  axes at  $45^\circ$  from the tetragonal  $a$  and  $b$  axes, respectively, and  $Z \equiv c$ . In this state, two types of structural domains exist in which the deuterons are ordered. In one type, the two deuterons associated with each  $\text{PO}_4$  tetrahedron are closer to the upper side of the group (i.e., toward the  $+c$  direction) while in the other type they are closer to the lower oxygens of the  $\text{PO}_4$  group. These two  $\text{D}_2\text{PO}_4^-$  configurations, with the accompanying ionic displacements in the complete ( $\text{K}^+-\text{D}_2\text{PO}_4^-$ ) molecule, give rise to the microscopic electric dipoles along the  $+c$  or  $-c$  directions. Macroscopic regions of similarly oriented ( $\text{K}^+-\text{D}_2\text{PO}_4^-$ ) molecules thus form the domains of electric polarization that comprise the ferroelectric phase. Most of the domains extend through the thickness of the crystal while others may end within the bulk of the crystal forming a layered domain pattern.<sup>15-17</sup>

## II. EXPERIMENTAL METHODS

The  $\text{KD}_2\text{PO}_4$  crystals were grown from an aqueous solution of 99.8%  $\text{D}_2\text{O}$  containing 99% isotopic purity  $\text{KD}_2\text{PO}_4$  and 5 mol % (vs  $\text{KD}_2\text{PO}_4$ ) of reagent grade  $\text{KH}_2\text{AsO}_4$ . Evaporation took place in a container under flowing argon gas to minimize deuterium-hydrogen exchange with the surrounding atmosphere. Crystals exhibiting the tetragonal symmetry of the high-temperature phase were selected for the polarization reversal experiments. Graphite electrodes were placed on the crystal faces perpendicular to the ferroelectric  $c$  axis of specimens having an approximately square cross-sectional area of  $2.5 \times 2.5 \text{ mm}^2$  and a thickness  $d$  of 1.5 mm along the  $c$  direction. With this geometry the strength of the electric field applied along the ferroelectric axis varied somewhat across the sample, however, the expression  $E = V/d$  was employed to provide nominal values of the field strength  $E$  from the applied voltage  $V$ . Samples were irradiated for several hours with 35-kV x rays at room temperature. The x-ray machine was operated with a Cu target and a current of 15 mA. ESR spectra were obtained with

an x-band superheterodyne spectrometer using a  $\text{TE}_{102}$  rectangular cavity in conjunction with an external low-temperature Dewar and temperature controller to attain temperatures stable to within  $\pm 1$  K. The sample and connecting wires were oriented inside a quartz tube such that the crystal could be rotated about its  $c$  axis for precise alignment in the magnetic field of the spectrometer. A pulse generator that could deliver variable width square high-voltage pulses of opposite polarity with rise times on the order of  $1 \mu\text{s}$  was constructed and used for polarizing and subsequent switching of the sample.

Irradiated  $\text{KD}_2\text{PO}_4\text{-KH}_2\text{AsO}_4$  crystals give ESR signals from a number of centers. In particular, the structure of the  $\text{AsO}_4^{4-}$  radical which is formed by the capture of an electron into a molecular orbital of the  $^{75}\text{As}$  ( $I = 3/2$ ) ion has been examined extensively.<sup>9</sup> The ESR spectrum of the  $\text{AsO}_4^{4-}$  center in ferroelectric  $\text{KD}_2\text{PO}_4$  is shown in Fig. 1 for the crystalline  $c$  axis perpendicular to the dc magnetic field and either the orthorhombic  $X$  or  $Y$  axis parallel to the magnetic field. This orientation of the crystal is such that the  $\text{AsO}_4$  tetrahedra having different angular orientations about the  $c$  axis are magnetically equivalent, while the two different  $\text{D}_2\text{AsO}_4^{4-}$  molecular configurations that give rise to the two oppositely directed domains of electrical polarization are magnetically inequivalent. As a result, the spectrum consists of two hyperfine quartets arising from the two types of domains. The maximum domain splitting is observed between the lowest-field lines of the two hyperfine quartets. The splitting between the corresponding lines of each hyperfine quartet at the three higher-field positions is not observed because of opposing  $\vec{g}$  and  $\vec{A}$  tensor effects.<sup>18</sup>

The ferroelectric nature of the splitting between the two lowest-field lines is evidenced by the effects of polarizing electric fields of opposite polarity on



FIG. 1. ESR spectrum of the  $\text{AsO}_4^{4-}$  free radical in  $\text{KD}_2\text{PO}_4$ -5 mol %  $\text{KH}_2\text{AsO}_4$  (DKDP-KDA) at 82 K with the  $^{75}\text{As}$  hyperfine transitions indicated by arrows, showing the line intensities  $I_1$  and  $I_2$  of the split lowest-field hyperfine component. Additional lines arising from other paramagnetic species also appear in the center of the spectrum ( $\vec{H} \parallel c$ ,  $\vec{H} \parallel X$  or  $Y$ ).

the line intensities  $I_1$  and  $I_2$  as denoted in Fig. 2. As the domains switch to the direction favored by the applied electric field, the number of  $\text{AsO}_4^{4-}$  centers in that domain type becomes greater, leading to an increase in the intensity of the associated ESR line and a corresponding decrease in the intensity of the other ESR line. A plot of the quantity

$$p(t) = (I_1 - I_2) / (I_1 + I_2), \quad (1)$$

as a function of the applied electric field at 82 K, yields a hysteresis loop similar to the ESR-monitored hysteresis loops that have been reported for other KDP-type systems.<sup>5,6,8</sup> These hysteresis effects show that  $p(t)$  represents the net fractional polarization of the crystal. Similarly, the quantities  $I_1 / (I_1 + I_2)$  and  $I_2 / (I_1 + I_2)$  may be taken to be proportional to polarizations of the two domain types. Therefore, when the crystal is switched from the polarized state for which  $I_1 \cong I_{1,\text{max}}$  and  $I_2 \cong 0$ , the function

$$g(t) = I_1 / (I_1 + I_2), \quad (2)$$

where  $I_1$  and  $I_2$  are the time-dependent line intensities, is proportional to the fractional polarization of the crystal that remains unswitched at time  $t$ . The function  $g(t)$  then provides the polarization versus time curve for the reversal process.

Two techniques were used to monitor the switching process. For each technique an unpolarized

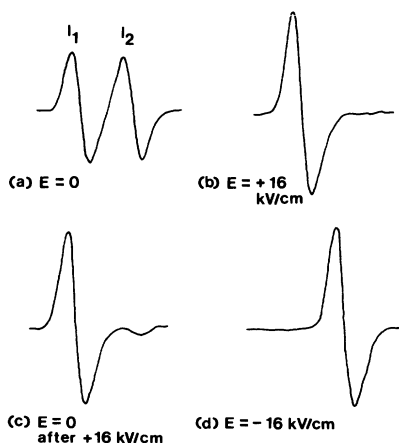


FIG. 2. Effect of an applied electric field on the split lowest-field hyperfine component of the  $\text{AsO}_4^{4-}$  radical in DKDP-KDA at 82 K showing (a) an equal intensity doublet for the initially unpolarized crystal, (b) presence of a single low-field line  $I_1$  after polarization in the  $+c$  direction, (c) growth of the weak  $I_2$  line on the right-hand side of the spectrum where the electric field is returned to zero, and (d) disappearance of line  $I_1$  and appearance of strong line  $I_2$  when the crystal is polarized in the opposite  $(-c)$  directions ( $\vec{H} \parallel c$ ,  $\vec{H} \parallel x$  or  $y$ ,  $\vec{E} \parallel c$ ).

crystal corresponding to Fig. 2(a) was first polarized with a high saturating electric field in one direction as in Fig. 2(b). The field was then returned to zero to allow spontaneous backswitching to occur as in Fig. 2(c). Finally, the electric field was reversed and the crystal polarized with time to the final state of Fig. 2(d). At low temperatures and low electric field strengths the polarization state changed slowly compared to the time required to scan through a spectrum, and so the switching process was monitored by repeatedly scanning through the spectrum of the two lines,  $I_1$  and  $I_2$ , presented in Fig. 2 at  $\sim 40$ -s intervals. At high temperatures and low electric field strengths the polarized state decayed too quickly to permit repeated scanning. To monitor the polarization for this case the spectrometer was set at the peak of the strongest of the low-field lines and the recorder was turned on during the polarization reversal so that the trace on the chart paper recorded the amplitude of the line  $I_1$  of Eq. (2). For this case, Eq. (2) assumes the form

$$g(t) = I_1 / I_1(0), \quad (3)$$

where  $I_1(0)$  is the amplitude for  $t = 0$ , and as before,  $I_2(0) \cong 0$ .

At high electric field strengths the polarization process is accompanied by an initial disturbance which momentarily mismatches the cavity followed by a rapid reversing of the polarization. As a result, the spectrum disappears and the switching could not be measured. A special technique involving pulsed electric fields was developed for monitoring the polarization reversal at high electric field strengths, and this is planned to be reported in a future subsequent publication.

### III. RESULTS

#### A. Short and long times

The time dependence of the polarization function  $g(t)$  given by Eq. (2) was measured for a series of temperatures  $T$  and electric field strengths  $E$  using the techniques described above. To display the results the logarithm of  $g(t)$  was plotted against both the time as shown in Fig. 3 and against the logarithm of the time as illustrated in Fig. 4. The semi-logarithmic plot for  $E = 10.0$  kV/cm and  $T = 82$  K exhibits a linear region at short times, less than a second, as indicated in Fig. 3, which corresponds more nearly to an exponential process of the form

$$g(t) \sim e^{-bt}. \quad (4)$$

The log-log plot for  $E = 7.3$  kV/cm and  $T = 106$  K presented in Fig. 4 is linear from times of 0.5 to about 9 min, indicative of a power-law behavior of

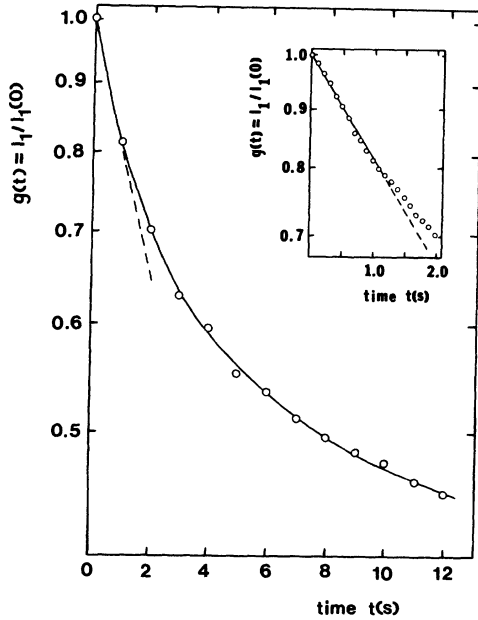


FIG. 3. Initial stage of the reversal process showing  $\log g(t)$  vs time. The inset presents an expansion of the region around  $t=0$  which shows that  $\log g(t)$  decreases linearly with time between 0 and 1 s ( $E=10.0$  kV/cm,  $T=82$  K).

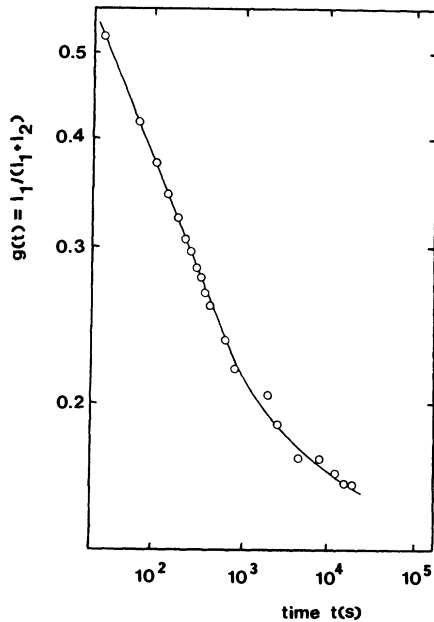


FIG. 4. Log-log plot of the polarization function  $g(t)$  vs time showing the linear region of the power-law dependence and the breakdown of the power-law behavior at longer times ( $E=7.3$  kV/cm,  $T=106$  K).

the form

$$g(t) \sim t^{-a}. \quad (5)$$

At still longer times, the power-law dependence breaks down and the polarization function  $g(t)$  approaches its final saturation value more slowly, as shown in the figure.

These results suggest that the application of a reversing electric field causes the polarization function  $g(t)$  to evolve in time from an initial value  $g(t) \sim 1$  to a final value  $g(t) \sim 0$  in the manner sketched in Fig. 5. This figure shows the following four regions of behavior for progressively increasing times: (1) an exponential law at very short times, (2) a transition region, (3) a power law at relatively long times, and (4) a more gradual approach to the final polarization state at very long times.

#### B. Power-law region

A particularly detailed study was made of the time decay of the polarization function in the power-law region where  $g(t)$  varies with time in accordance with Eq. (5). Measurements made at 82 K for a series of electric field strengths from 4.0 to 8.0 kV/cm exhibit the linear behavior illustrated in Fig. 6 for each value of  $E$ . We see from the figure that  $g(t)$  has progressively smaller values for the shortest time shown, namely 27 s, which means that for shorter times  $g(t)$  decreases more rapidly for in-

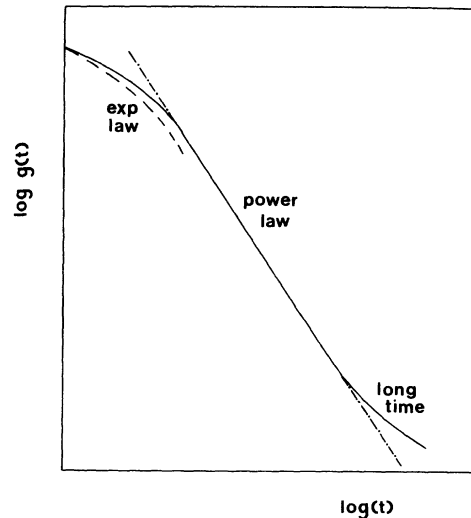


FIG. 5. Different regions of behavior of the polarization function  $g(t)$  represented by a solid line (—). (a) Exponential time dependence at very short times (---) and (—), (b) power law at intermediate times (-·-·-) and (—), and (c) unknown time dependence at very long times (—).

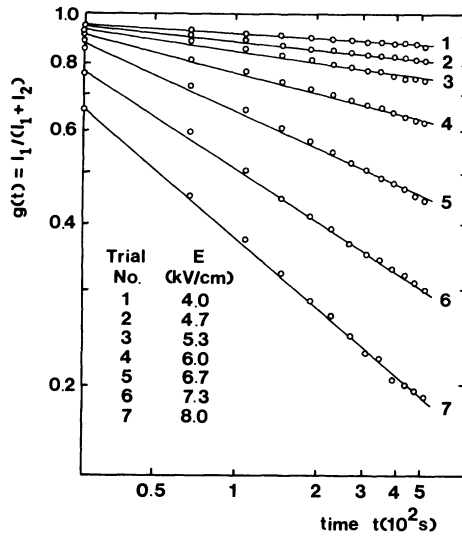


FIG. 6. Log-log plot of the polarization function  $g(t)$  vs the time  $t$  for reversal field strengths at a temperature of 82 K. The linearity of the curves indicates a power-law behavior, and the decrease in the value of  $g(t)$  with increasing electric field strength for the shortest time shown indicates that the short-time decay becomes more rapid with increasing  $E$ .

creasing values of  $E$ . The linearity of the curves in Fig. 6 demonstrates that the power-law behavior of Eq. (5) is closely followed for the relatively long-time period from 0.5 to 9 min. In addition, we see from the figure that the magnitudes of the slopes of the lines become greater with increasing electric field strength, hence in the power-law region  $g(t)$  continues to decrease more rapidly for increasing values of  $E$ .

To obtain a quantitative measure of the way  $g(t)$  changes with electric field strength in the linear region, a semilogarithmic plot was made of the slopes of the lines in Fig. 6, and the results presented in Fig. 7 show that the power-law exponent  $a$  is an exponential function of the electric field of the form

$$a(E) \sim e^{\alpha E}, \quad (6)$$

with

$$\alpha = 0.67 \pm 0.2, \quad (7)$$

measured in cm/kV. Thus we have an analytic expression for the electric field dependence in the power-law region at a temperature of 82 K.

A similar approach was used to ascertain how  $g(t)$  depends upon the temperature for a particular electric field strength  $E$ . Measurements were made of the time dependence of  $g(t)$  for a series of temperatures between 88 and 113 K at the fixed electric field strength  $E = 4.0$  kV/cm, and they are dis-

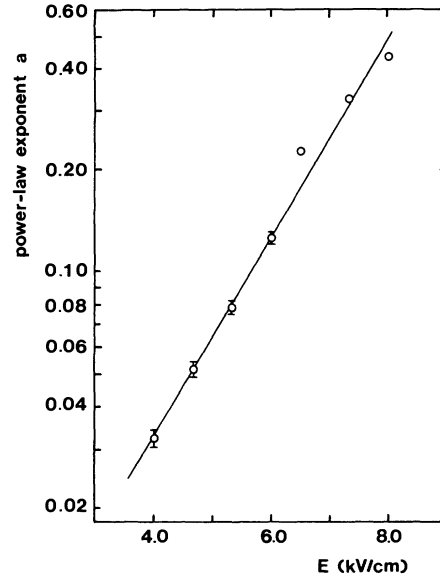


FIG. 7. Semilogarithmic plot of the electric field dependence of the power-law exponent  $a$  obtained from the slopes of the lines in Fig. 6 for the temperature of 82 K.

played in Fig. 8. The initial value of  $g(t)$  for each curve at 27 s was lower for progressively higher temperatures indicating that the short-time decrease of  $g(t)$  with time is more rapid for increasing temperatures. The linearity of the curves shows that the power-law behavior is again obeyed for times between 0.5 and 9 min.

To ascertain the explicit temperature dependence of the polarization function  $g(t)$ , a semilogarithmic plot was made of  $\log g(t)$  vs  $1/T$ , and the resulting straight line presented in Fig. 9 shows that the power-law exponent  $a$  in Eq. (5) varies exponentially with  $1/T$  in accordance with the expression

$$a(T) \sim e^{-\beta/T}, \quad (8)$$

where

$$\beta = 0.73 \pm 0.04 \quad (9)$$

measured in units of k. This provides us with an analytic expression for the temperature dependence in the power-law region at an electric field strength of 4.0 kV/cm.

#### IV. DISCUSSION

The short-time data in Fig. 3 were obtained for  $E = 10.0$  kV/cm and  $T = 82$  K, and the long-time data in Fig. 4 were for the conditions  $E = 7.3$  kV/cm and  $T = 106$  K. Additional measurements under other conditions of  $E$  and  $T$  presented in Figs.

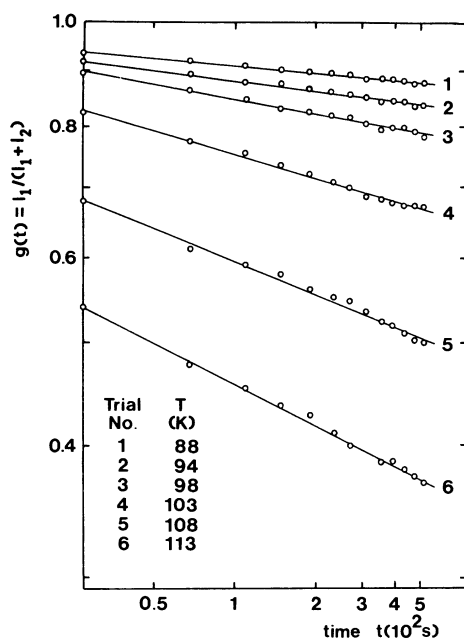


FIG. 8. Log-log plot of the polarization function  $g(t)$  vs the time  $t$  for several temperatures at an electric field strength of 4.0 kV/cm. The linearity of the curves indicates a power-law behavior, and the decrease in the value of  $g(t)$  with increasing temperatures for the shortest time shown indicates that the short-time decay becomes more rapid with increasing temperature.

6 and 8 show that increasing the value of either the electric field or the temperature causes the polarization function  $g(t)$  to decrease more rapidly with time in both the short-time exponential region and in the longer-time power-law region. The coefficients  $\alpha$  and  $\beta$  of Eqs. (7) and (9) were evaluated and provide a quantitative measure of the electric field and temperature dependence, respectively, of the power-law exponent  $a$  of Eq. (5). It is believed that  $\alpha$  varies with the temperature and  $\beta$  varies with the electric field strength, and these dependences are being determined.

The results presented in this paper were limited to

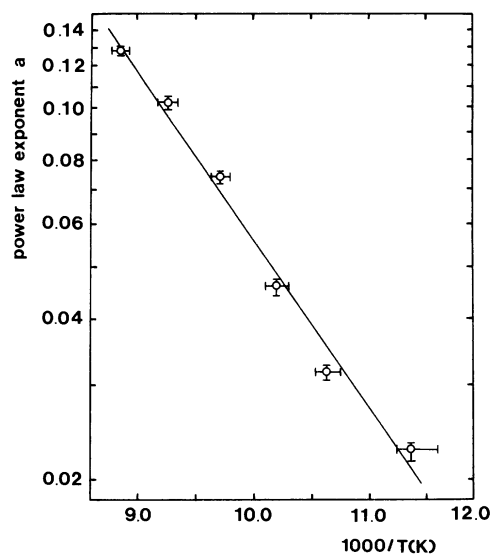


FIG. 9. Semilogarithmic plot of the temperature dependence of the power-law exponent  $a$  in a constant field on the reciprocal temperature obtained from the 4.0-kV/cm reversing field. Slopes of the lines in Fig. 8 for the reversing electric field strength of 4.0 kV/cm.

relatively low electric field strengths because higher-field strengths disturbed the cavity and prevented data from being obtained. More recently, a pulsed electric field method has been developed which permits data to be obtained at higher electric field strengths, and this is planned to be reported in a future subsequent publication. Further work is also in progress on the interpretation of these results with respect to the usual theories of ferroelectric switching by the nucleation of reversed domains and their subsequent expansion.<sup>19,20</sup>

#### ACKNOWLEDGMENT

This work was supported by the NSF under Grant No. ISP-80-11451.

\*Based on a thesis submitted in partial fulfillment of the requirements of the Ph.D. at the University of South Carolina.

<sup>1</sup>E. Fatuzzo and W. J. Merz, *Ferroelectricity* (North-Holland, Amsterdam, 1967), Chap. 6.

<sup>2</sup>M. E. Lines and A. E. Glass, *Principles and Applications of Ferroelectrics and Related Materials* (Clarendon, Oxford, 1977), Chap. 16.

<sup>3</sup>F. Jona and G. Shirane, *Ferroelectric Crystals* (Pergamon, New York, 1962).

<sup>4</sup>R. C. DuVarney and R. P. Kohin, *Phys. Rev. Lett.* **20**, 259 (1968).

<sup>5</sup>R. D. Truesdale, H. A. Farach, and C. P. Poole, Jr., *Phys. Rev. B* **22**, 365 (1980).

<sup>6</sup>N. S. Dalal, C. A. McDowell, and R. Srinivasan, *Phys. Rev. Lett.* **25**, 823 (1970).

<sup>7</sup>R. Blinc and P. Cevc, *Solid State Commun.* **6**, 635 (1968).

<sup>8</sup>J. Hukuda, H. Hanafusa, and T. Kawano, *J. Phys. Soc. Jpn.* **36**, 1043 (1974).

- <sup>9</sup>N. S. Dalal, J. A. Hebden, D. E. Kennedy, and C. A. McDowell, *J. Chem. Phys.* **66**, 4425 (1977).
- <sup>10</sup>R. D. Truesdale, C. P. Poole, Jr., and H. A. Farach, *Phys. Rev. B* **25**, 474 (1982).
- <sup>11</sup>R. J. Nelmes, V. R. Eiriksson, and K. D. Rouse, *Solid State Commun.* **11**, 1261 (1972).
- <sup>12</sup>J. Nakano, Y. Shiozaki, and E. Nokamura, *J. Phys. Soc. Jpn.* **34**, 1423 (1973).
- <sup>13</sup>R. J. Nelmes, G. M. Meyer, and J. E. Tiballs, *J. Phys. C* **15**, 59 (1982).
- <sup>14</sup>R. J. Nelmes, *Phys. Status Solidi B* **52**, K89 (1972).
- <sup>15</sup>J. L. Bjorkstam and R. E. Oettel, in *Proceedings of the International Meeting on Ferroelectricity, Prague, 1966*, edited by V. Dvorak, A. Fouskova, and P. Glogar (Fyzikalni Ustav. Czechoslovakian Acad. Sci., Lumumbova, Prague, 1966), Vol. II, p. 91.
- <sup>16</sup>S. D. Toshev, *Kristallografiya* **8**, 680 (1963) [*Sov. Phys.—Crystallogr.* **8**, 541 (1964)].
- <sup>17</sup>I. Bornarel, *Ferroelectrics* **2**, 197 (1975).
- <sup>18</sup>N. S. Dalal, C. A. McDowell, and R. Srinivasan, *Mol. Phys.* **24**, 417 (1972).
- <sup>19</sup>A. G. Chynoweth, *Phys. Rev.* **110**, 1316 (1958).
- <sup>20</sup>H. H. Weider, *J. Appl. Phys.* **31**, 180 (1960).